NASA TECHNICAL NOTE

NASA TN D-3879

NASA TN D-3879

INVESTIGATION OF FATIGUE CRACK GROWTH IN Ti-8Al-1Mo-1V (DUPLEX-ANNEALED) SPECIMENS HAVING VARIOUS WIDTHS

by C. Michael Hudson

Langley Research Center
Langley Station, Hampton, Va.

NATIONAL AERONAUTICS AND SPACE ADMINISTRATION • WASHINGTON, D. C. • MARCH 1967

NASA TN D-3879

INVESTIGATION OF FATIGUE CRACK GROWTH IN Ti-8Al-1Mo-1V (DUPLEX-ANNEALED) SPECIMENS HAVING VARIOUS WIDTHS

By C. Michael Hudson

Langley Research Center
Langley Station, Hampton, Va.

NATIONAL AERONAUTICS AND SPACE ADMINISTRATION

For sale by the Clearinghouse for Federal Scientific and Technical Information
Springfield, Virginia 22151 – CFSTI price $3.00

INVESTIGATION OF FATIGUE CRACK GROWTH IN Ti-8Al-1Mo-1V (DUPLEX-ANNEALED) SPECIMENS HAVING VARIOUS WIDTHS

By C. Michael Hudson
Langley Research Center

SUMMARY

Axial-load fatigue-crack-propagation tests were conducted on 2-, 4-, 8-, and 20-inch-wide (5.1-, 10.2-, 20.3-, and 50.8-cm) sheet specimens made of Ti-8Al-1Mo-1V (duplex-annealed) titanium alloy to study the effect of specimen width on fatigue crack growth. Both longitudinal- and transverse-grain specimens having a width of 8 inches (20.3 cm) were studied. Tests were conducted at a mean stress of 25 ksi (173 MN/m^2) and at five alternating stresses with amplitudes ranging from 2 to 25 ksi (14 to 173 MN/m^2). At a given stress level, there was relatively little difference between the fatigue-crack-growth curves for different specimen widths. Schijve et al. (Rept. NLR-TR M.2142) found a similar result in tests on clad 2024-T3 aluminum-alloy specimens. The resulting data were successfully correlated by using both Paris' and a slightly modified form of McEvily and Illg's crack-propagation analyses (see book entitled "Fatigue – An Interdisciplinary Approach," Syracuse Univ. Press, 1964, and NACA TN 4394, respectively). A simple power function relating rate and stress-intensity factor was empirically adjusted to fit the test data.

Wilhem (ASTM Preprint No. 38, 1966) found the transition of the specimen fracture surfaces from the tensile to the shear mode to be associated with the change in slope of the semilog plot of rate of crack growth against stress-intensity factor; however, inspection of the fracture surfaces of specimens tested in the present investigation showed no such correlation.

Cracks grew slightly faster in the transverse grain direction than in the longitudinal direction.

INTRODUCTION

The fatigue process includes three general phases: crack initiation, crack propagation, and residual static strength. The crack propagation phase frequently occupies a major portion of the process. Consequently, parameters which affect fatigue crack growth

can have an important effect on total fatigue behavior. One parameter which may affect fatigue crack growth is the width of the part through which the cracks propagate. The present investigation was conducted to study the effects of this parameter. Axial-load fatigue-crack-growth tests were conducted on sheet Ti-8Al-1Mo-1V (duplex-annealed) titanium-alloy specimens. (This alloy was selected because of its potential for use in supersonic aircraft construction.) These specimens ranged in width from 2 to 20 inches (5.1 to 50.8 cm). Tests were conducted at one mean stress and five alternating stresses for each specimen width.

The data were correlated by using both McEvily and Illg's (ref. 1) and Paris' (ref. 2) crack-growth analyses. In reference 3, Wilhem reported a correlation between the stress-intensity factor and the transition of the fracture surfaces from a tensile to a shear mode. The fracture surfaces of the specimens tested in this investigation were inspected to see whether a similar correlation existed. The effects of grain direction on fatigue crack growth were also investigated.

SYMBOLS

The units used for the physical quantities defined in this paper are given both in the U.S. Customary Units and in the International System of Units (SI). Factors relating the two systems are given in reference 4 and those used in the present investigation are presented in appendix A.

a	one-half of the total length of a central symmetrical crack, in. (cm)
C,C*	constant in crack propagation equation accounting for mean load, loading frequency, and environment
E	Young's modulus of elasticity, ksi (GN/m^2)
e	elongation in 2-inch (5.1-cm) gage length, percent
Δk	range of fluctuation of stress-intensity factor, ksi-$in^{1/2}$ $\left(MN/m^{3/2}\right)$
K_{TN}	Neuber technical stress-concentration factor
K_w	finite width factor (see appendix B)

k_{max} stress-intensity factor corresponding to maximum stress, ksi-in$^{1/2}$ $(MN/m^{3/2})$

k_{min} stress-intensity factor corresponding to minimum stress, ksi-in$^{1/2}$ $(MN/m^{3/2})$

L denotes longitudinal-grain specimen

N number of cycles

n exponent in fatigue-crack-growth equation

P_a amplitude of alternating load, kips (N)

P_m mean load, kips (N)

P_{max} maximum load, $P_m + P_a$, kips (N)

P_{min} minimum load, $P_m - P_a$, kips (N)

R ratio of minimum stress to maximum stress

S'_a amplitude of alternating net stress, $P_a/(w - x)t$, ksi (MN/m^2)

S''_a amplitude of instantaneous alternating net stress, $P_a/(w - 2a)t$, ksi (MN/m^2)

S'_m mean net stress, $P_m/(w - x)t$, ksi (MN/m^2)

S_{max} maximum gross stress, P_{max}/wt, ksi (MN/m^2)

S''_{max} instantaneous maximum net stress, $P_{max}/(w - 2a)t$, ksi (MN/m^2)

S_{min} minimum gross stress, P_{min}/wt, ksi (MN/m^2)

T denotes transverse-grain specimen

t specimen thickness, in. (mm)

w	specimen width, in. (cm)
x	length of crack-starter notch, in. (cm)
α	tangent correction factor for finite width of panel
ρ_e	effective radius of curvature at tip of a fatigue crack, in. (cm)
σ_u	ultimate tensile strength, ksi (MN/m^2)
σ_y	yield strength (0.2-percent offset), ksi (MN/m^2)

SPECIMENS

All specimens were made from Ti-8Al-1Mo-1V (duplex-annealed) titanium-alloy sheet 0.050 inch (1.27 mm) in thickness. All the material used in this investigation was obtained from the same mill heat. Tensile properties and the nominal chemical composition of the material are listed in table I. Details of the duplex-annealed heat treatment are also presented in table I. The configurations of the crack propagation specimens are shown in figure 1. The width and length of the specimens are as follows:

Width		Length	
in.	cm	in.	cm
2	5.1	12	31
4	10.2	12	31
8	20.3	24	61
20	50.8	40	102

The 2-, 4-, and 20-inch-wide (5.1-, 10.2-, and 50.8-cm) specimens were made with the longitudinal axis of the specimen parallel to the grain of the sheet. The 8-inch-wide (20.3-cm) specimens were made with the longitudinal axis of the specimens normal to the grain of the sheet. The width at the ends of the 20-inch-wide (50.8-cm) specimens was reduced to accommodate the 12-inch (31-cm) grips available on the testing machines. Doubler plates, 3/32 inch (2.38 mm) thick, were bonded to the ends of these 20-inch (50.8-cm) specimens (by using an unfilled epoxy resin) to reduce the stress. The interior ends of these doubler plates were scarfed to zero thickness in 2 inches (5.1 cm) to provide gradual load transfer from the doublers to the test specimens.

A 0.1-inch-long (0.25-cm) central notch was cut into the center of each specimen to initiate the fatigue cracks. These notches were cut by using a spark discharge

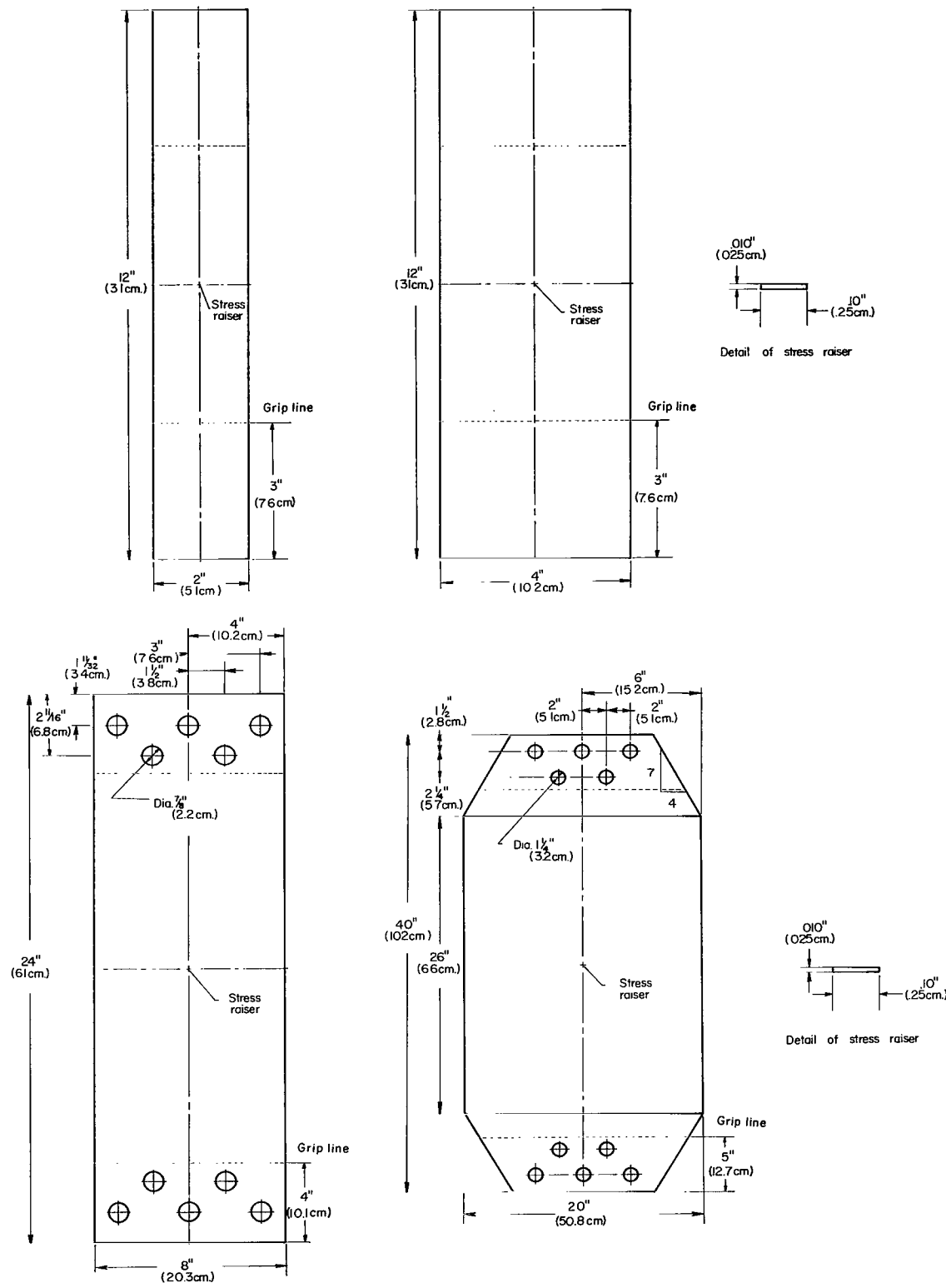

Figure 1.- Specimen configurations. Specimen thickness, 0.050 inch (1.27 mm).

process. The heat generated by this process is localized and was not expected to affect the bulk of the material through which the fatigue cracks propagated.

To mark intervals along the path of the crack, a reference grid (ref. 5) was photographically printed on the surface of the specimens. Some specimens bearing the grid were subjected to tensile tests and metallographic examination, which indicated that the grid had no detrimental effect on the material.

TESTING MACHINES

Two types of axial-load fatigue-testing machines were employed in this investigation: a ±20-kip-capacity (89-kN) subresonant machine which had an operating frequency of 1800 cpm (30 Hz) and a combination hydraulic and subresonant machine. The combination machine could apply alternating loads up to 66 kips (294 kN) hydraulically or 39 kips (173 kN) subresonantly. The operating frequencies were 40 to 60 cpm (0.7 to 1 Hz) for the hydraulic unit and approximately 820 cpm (13.7 Hz) for the subresonant unit.

Loads were monitored continuously by measuring the output of a strain-gage bridge cemented to a dynamometer in series with the specimen. The maximum error anticipated for this monitoring system was ±1 percent.

TEST PROCEDURE

Axial-load fatigue tests were conducted under a positive mean stress of 25 ksi (173 MN/m^2). Alternating stresses ranged from 2 to 25 ksi (14 to 173 MN/m^2). Both the mean and the alternating stresses were based on the original net area of the specimens. The mean load and the amplitude of the alternating loads were kept constant throughout the crack-propagation portion of each test. Fatigue cracks were sometimes initiated at an alternating stress level slightly higher than the level used in the crack growth portion of the test to expedite testing. The alternating stress was subsequently reduced to the desired level after crack initiation.

Fatigue crack growth was observed through a 10-power monocular telescope while illuminating the specimen with stroboscopic light. The number of cycles required to propagate the crack to each grid line was recorded so that the crack growth rates could be determined. Tests were terminated when the cracks reached a predetermined crack length.

In all tests, specimens were clamped between lubricated guides (ref. 6) to prevent buckling and out-of-plane vibrations during testing. Light oil was used to lubricate the surfaces of the specimens and guides. A 1/2-inch-wide (1.27-cm) slot was made across the width of the guide plate to allow visual observation of the crack growth region.

RESULTS AND DISCUSSION

The results of the fatigue-crack-propagation tests are presented in table II, which gives the number of cycles required to grow the crack from a half-length a of 0.15 inch (0.38 cm) to the specified half-lengths. The number of cycles given in table II is the mean number of cycles required to propagate cracks of equal length on both sides of the central notch. Included in table II are data from reference 7 for longitudinal-grain sheet specimens having a width of 8 inches (20.3 cm). The material tested in both this investigation and reference 7 was from the same mill heat.

The ratios of the clear height to the specimen width were somewhat small for the 4- and 20-inch-wide (10.2- and 50.8-cm) specimens (1.5 and 1.3, respectively). These small ratios were not expected to affect crack growth significantly in this investigation, however, because the crack lengths were relatively short in comparison with the specimen widths ($2a/w < 0.5$). Successful correlation (to be shown subsequently) of the data from these specimens with the data from the 2- and 8-inch-wide (5.1- and 20.3-cm) specimens (having ratios of clear height to width of 3 and 2, respectively) indicated that there was no significant effect.

The cracks generally grew symmetrically about the specimen center line, with eccentricities seldom exceeding 0.05 inch (1.27 mm). Fatigue-crack-growth rates were determined graphically by taking the slopes of the fatigue-crack-growth curves (plotted on a linear scale) at various crack lengths. The fatigue-crack-growth data are presented in figure 2. Included in figure 2 are the data for the 8-inch-wide (20.3-cm) longitudinal-grain sheet specimens (ref. 7). At a given stress level there was relatively little difference between the curves for different specimen widths. Schijve et al. (ref. 8) also found, in tests on clad 2024-T3, that specimen width had a relatively slight effect on crack propagation.

For the 8-inch-wide (20.3-cm) specimens, the cracks consistently propagated more rapidly in the transverse grain direction than in the longitudinal direction. However, the differences between these curves were slight at all five stress levels.

The fatigue-crack-growth data were analyzed by using a modified form of McEvily and Illg's method (ref. 1). The principle behind this method is that the rate of fatigue crack growth is an explicit function of the product of the theoretical stress-concentration factor for the crack (K_{TN}) and the instantaneous maximum net stress (S''_{max}). In the present investigation, the theoretical stress-concentration factors for cracks were computed by using the following equation (see appendix B):

$$K_{TN} = 1 + 2K_w\sqrt{a/\rho_e} \tag{1}$$

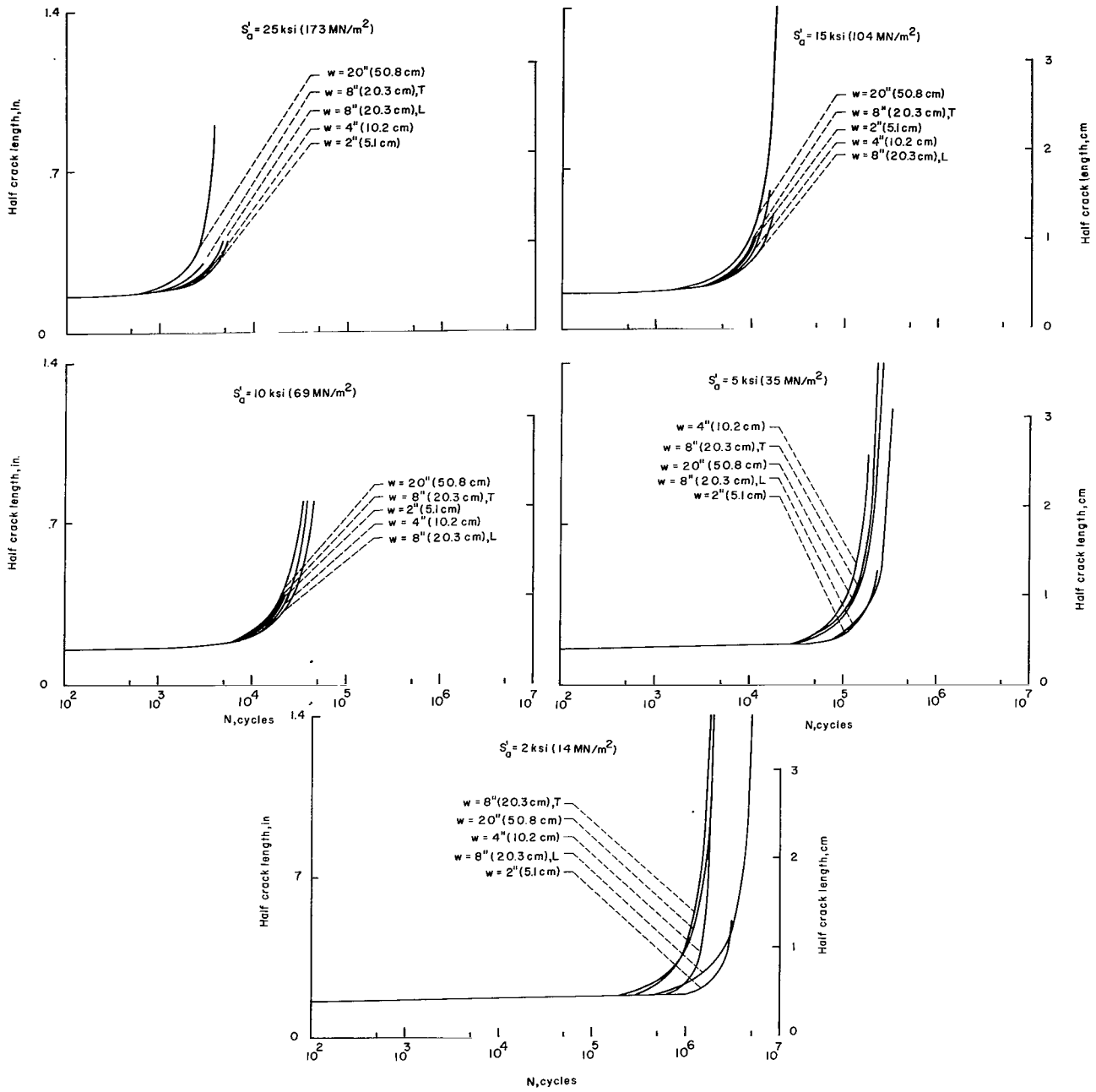

Figure 2.- Fatigue-crack-propagation curves for Ti-8Al-1Mo-1V (duplex-annealed) specimens tested at S'_m = 25 ksi (173 MN/m^2).

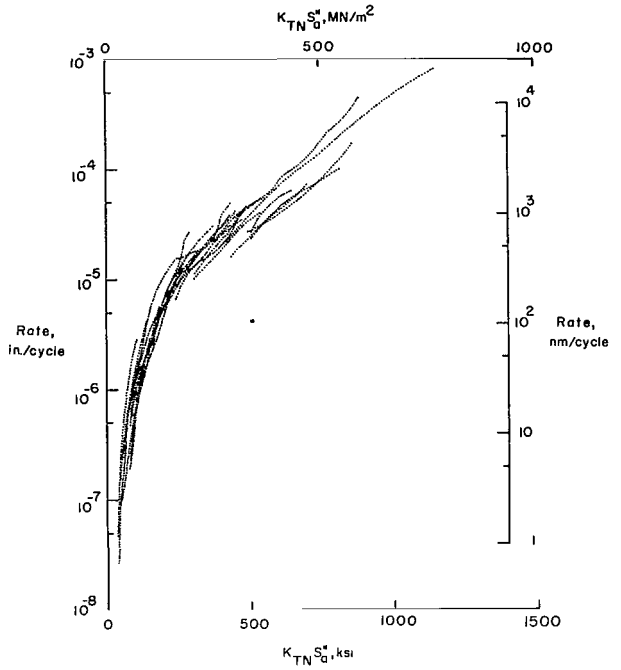

Figure 3.- Variation of fatigue-crack-growth rate with $K_{TN}S''_a$ for all specimen widths. Each curve is an individual test.

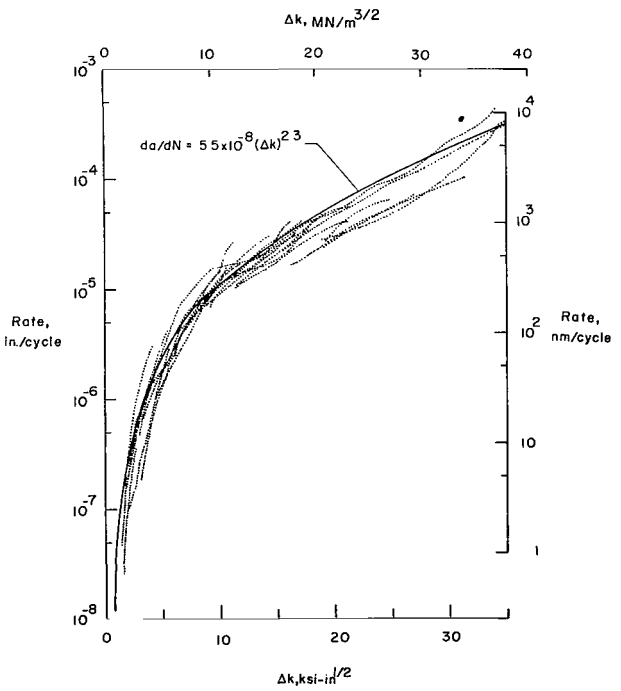

Figure 4.- Variation of fatigue-crack-growth rate with Δk for all specimen widths. Each curve is an individual test.

A value of $\sqrt{\rho_e}$ equal to 0.04 in$^{1/2}$ (0.20 mm$^{1/2}$) was selected by trial-and-error adjustment of the data.

McEvily and Illg's method correlated the crack-growth data from tests conducted at constant stress ratios (R = 0 and -1) quite well for two aluminum alloys and one stainless steel (refs. 1, 9, and 10). However, the data from the present investigation were obtained from constant-mean-stress tests, which meant that for a given specimen width each test was conducted at a different stress ratio. When the test results were analyzed by using S''_{max}, very poor correlation of the data resulted. Substitution, however, of the instantaneous-stress amplitude S''_a in place of S''_{max} resulted in good correlation of the data (fig. 3) and thereby indicated that alternating-stress amplitude was a predominant factor affecting fatigue crack growth. Frost and Dugdale (ref. 11) reported a similar finding from tests on sheet specimens made of an aluminum alloy, mild steel, and copper.

The fatigue-crack-growth data were also analyzed by using Paris' stress-intensity analysis method (ref. 2). The data fell within a reasonably small scatter band on a semilog plot of rate of crack growth against Δk. (See fig. 4.) The following relationship having the form of equation (C1) in appendix C

$$\frac{da}{dN} = C^*(\Delta k)^n \qquad (2)$$

was adjusted to fit the test data reasonably well. The exponent n and the constant C^* were empirically determined to equal

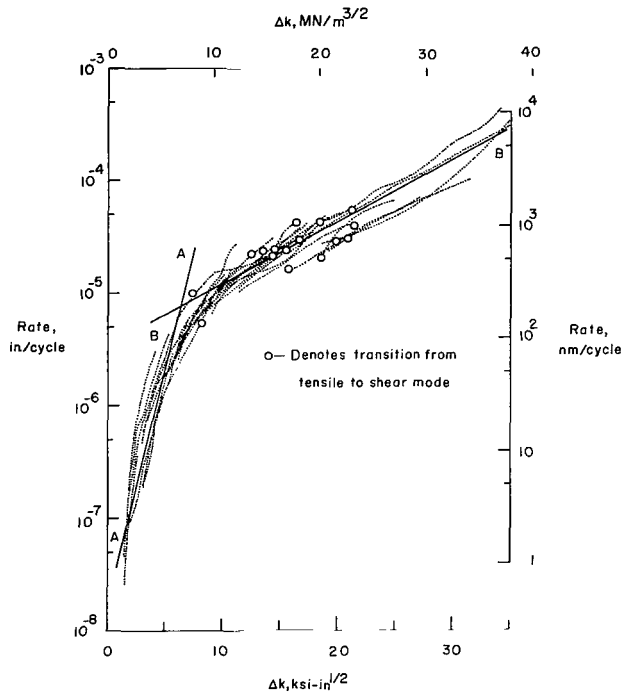

Figure 5.- Variation of rate with Δk showing data at start of transition from tensile to shear mode.

2.3 and 5.5×10^{-8}, respectively. Liu (refs. 12 and 13) and McEvily and Boettner (ref. 14) have shown that the exponent n can take on values ranging from 2 to 6 depending upon the material, the magnitude of the stress-intensity factor, and the stress condition (plane stress or plane strain).

Wilhem (ref. 3) inspected the fracture surfaces of fatigue-tested specimens and determined the crack lengths at which the transition from the tensile mode (fracture surface normal to the sheet) to a shear mode (fracture surface 45° to the thickness direction) began. He found a relationship between the Δk at these transition crack lengths and the Δk associated with the change in slope of the semilog plot of the rate against Δk. The fracture surfaces of the specimens tested in the present investigation were inspected to determine whether a similar relationship existed. The values of Δk and the corresponding rates of crack growth at these transition crack lengths (table III) are shown as circles in figure 5. The data from figure 4 have been approximated by two straight lines, A-A and B-B, in figure 5. The fact that the value of Δk at the intersection of these lines was considerably lower (by a factor of about 2) than the average value of Δk for the transition data indicates that no relationship exists for Ti-8Al-1Mo-1V (duplex-annealed) specimens.

The crack surfaces changed from the tensile mode to single, double, or dual (single at one end of the crack and double at the other) shear modes. (See table III.) No relationship between the type (single, double, or dual) of shear mode and the value of S'_a was apparent.

CONCLUDING REMARKS

Axial-load fatigue-crack-propagation tests were conducted on 2-, 4-, 8-, and 20-inch-wide (5.1-, 10.2-, 20.3-, and 50.8-cm) sheet specimens made of Ti-8Al-1Mo-1V (duplex-annealed) titanium alloy. These tests were conducted at a mean stress of 25 ksi (173 MN/m^2) and at five alternating stress amplitudes ranging from 2 to 25 ksi (14 to 173 MN/m^2). Tests were conducted at the same initial net-section stress levels for each

specimen width to make the resulting data comparable. Analysis of the test results supports the following general conclusions:

1. At a given stress level, the differences between the fatigue-crack-propagation curves for different specimen widths were not significant. Schijve et al. (Rept. NLR-TR M.2142) reported a similar finding in tests on clad 2024-T3 aluminum-alloy specimens.

2. Fatigue cracks grew slightly faster in the transverse grain direction than in the longitudinal direction.

3. The data were successfully correlated by using a modified form of McEvily and Illg's fatigue-crack-growth analysis (NACA TN 4394). The instantaneous alternating stress amplitude was substituted for the instantaneous maximum stress in their analysis. (Use of the instantaneous net stress resulted in poor correlation of the data.) These findings are consistent with those of Frost and Dugdale (J. Mech. Phys. Solids, vol. 6, no. 2, 1958), who found that alternating stress was a predominant factor affecting fatigue crack growth. Additional research on mean-stress effects would aid even further in understanding the fatigue-crack-growth phenomenon.

4. The data were successfully correlated by using Paris' analysis method. (See book entitled "Fatigue – An Interdisciplinary Approach," Syracuse Univ. Press, 1964.) A simple power function relating rate and stress-intensity factor Δk was empirically adjusted to fit the test data. The exponent of this power function was 2.3. Previous investigations have reported values of the exponent ranging from 2 to 6 depending upon material, the magnitude of Δk, and the stress condition (plane stress or plane strain).

5. The crack surfaces changed from the tensile fracture mode to single, double, or dual (single at one end of the crack and double at the other) shear fracture modes. No relationship between the type (single, double, or dual) of shear mode and the amplitude of the alternating net stress was apparent.

6. Wilhem (ASTM Preprint No. 38, 1966) found the transition of the specimen fracture surfaces from the tensile to the shear mode to be associated with the change in slope of the semilog plot of rate of crack growth against stress-intensity factor; however, inspection of the fracture surfaces of specimens tested in the present investigation showed no such correlation.

Langley Research Center,
National Aeronautics and Space Administration,
Langley Station, Hampton, Va., October 31, 1966,
126-14-03-01-23.

APPENDIX A

CONVERSION OF U.S. CUSTOMARY UNITS TO SI UNITS

The International System of Units was adopted by the Eleventh General Conference on Weights and Measures, Paris, October 1960. (See ref. 4.) Factors required for converting the U.S. Customary Units used herein to the International System of Units (SI) are given in the following table:

Physical quantity	U.S. Customary Unit	Conversion factor (*)	SI Unit
Force	lb	4.448	newtons (N)
	kip	4448	
Frequency	cpm	0.01667	hertz (Hz)
Length	in.	0.0254	meters (m)
Pressure	ksi	6.9×10^6	newtons/meter^2 (N/m^2)
Temperature . . .	^oF	$\frac{5}{9}(F + 459.67)$	degrees Kelvin (^oK)

*Multiply value given in U.S. Customary Unit by conversion factor to obtain equivalent value in SI Unit.

Prefixes to indicate multiples of units are as follows:

Prefix	Multiple
giga (G)	10^9
mega (M)	10^6
kilo (k)	10^3
centi (c)	10^{-2}
milli (m)	10^{-3}
nano (n)	10^{-9}

APPENDIX B

McEVILY AND ILLG'S FATIGUE-CRACK-GROWTH ANALYSIS

McEvily and Illg's analysis (refs. 1 and 9) proposed that the rate of fatigue crack propagation at $R = 0$ and -1 was an explicit function of the product of the instantaneous maximum net stress (S''_{max}) and the theoretical stress-concentration factor for the crack (K_{TN}). A boundary condition that fatigue crack growth could not occur at values of $K_{TN}S''_{max}$ less than the fatigue limit (at the appropriate R value) of the unnotched material was proposed. McEvily and Illg developed a semiempirical equation which fits the test data reasonably well. However, this equation was not applicable to the constant-mean-stress data generated in the present investigation.

In the present investigation, the theoretical stress-concentration factors for cracks were computed by using the equation developed in reference 15. For the crack-propagation case, this equation has the form

$$K_{TN} = 1 + 2K_w\sqrt{a/\rho_e} \tag{B1}$$

where K_w is a finite width factor determined from photoelastic studies by Dixon (ref. 16), a is one-half the length of the crack, and ρ_e is the effective radius of curvature at the tip of the fatigue crack. A plot of K_w against $2a/w$ is given in figure B1.

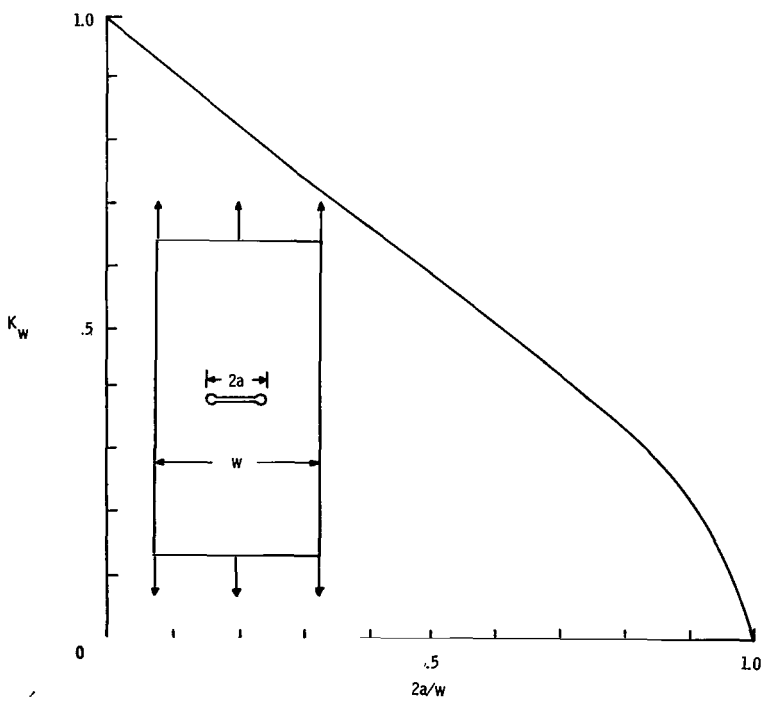

Figure B1.- Dixon's finite width correction.

APPENDIX C

PARIS' FATIGUE-CRACK-GROWTH ANALYSIS

Paris' method (ref. 2) hypothesized that the rate of fatigue crack propagation was a function of the stress-intensity factor. Paris found the following relationship between the rate of fatigue crack growth and the stress-intensity factor:

$$\frac{d(2a)}{dN} = C(\Delta k)^n \tag{C1}$$

where

$$\Delta k = k_{max} - k_{min} \tag{C2}$$

and C is a constant which is proposed to incorporate the effects of mean load, loading frequency, and environment. Paris found that a value of $n = 4$ fits the broad trend of the data.

For centrally cracked specimens subjected to a uniformly distributed axial load,

$$k_{max} = S_{max}\sqrt{a}\,\alpha \tag{C3}$$

and

$$k_{min} = S_{min}\sqrt{a}\,\alpha \tag{C4}$$

The term α is a factor which corrects for the finite width of the specimen and is given by

$$\alpha = \sqrt{\frac{w}{\pi a}\tan\frac{\pi a}{w}} \tag{C5}$$

The term S_{max} is the maximum gross stress in the cycle, and S_{min} is the minimum gross stress in the cycle.

REFERENCES

1. McEvily, Arthur J., Jr.; and Illg, Walter: The Rate of Fatigue-Crack Propagation in Two Aluminum Alloys. NACA TN 4394, 1958.

2. Paris, Paul C.: The Fracture Mechanics Approach to Fatigue. Fatigue – An Interdisciplinary Approach, John J. Burke, Norman L. Reed, and Volker Weiss, eds., Syracuse Univ. Press, 1964, pp. 107-132.

3. Wilhem, D. P.: Investigation of Cyclic Crack Growth Transitional Behavior. Preprint No. 38, Am. Soc. Testing Mater., June 1966.

4. Mechtly, E. A.: The International System of Units – Physical Constants and Conversion Factors. NASA SP-7012, 1964.

5. Hudson, C. Michael: Fatigue-Crack Propagation in Several Titanium and Stainless-Steel Alloys and One Superalloy. NASA TN D-2331, 1964.

6. Bruggeman, W. C.; and Mayer, M., Jr.: Guides for Preventing Buckling in Axial Fatigue Tests of Thin Sheet-Metal Specimens. NACA TN 931, 1944.

7. Hudson, C. Michael: Studies of Fatigue Crack Growth in Alloys Suitable for Elevated-Temperature Applications. NASA TN D-2743, 1965.

8. Schijve, J.; Nederveen, A.; and Jacobs, F. A.: The Effect of the Sheet Width on the Fatigue Crack Propagation in 2024-T3 Alclad Material. Rept. NLR-TR M.2142, Natl. Lucht- en Ruimtevaartlab. (Amsterdam), Mar. 1965.

9. Illg, Walter; and McEvily, Arthur, J., Jr.: The Rate of Fatigue-Crack Propagation for Two Aluminum Alloys Under Completely Reversed Loading. NASA TN D-52, 1959.

10. Hudson, C. Michael: Fatigue-Crack Propagation and Residual Static Strength of PH 15-7 Mo (TH 1050) Stainless Steel. NASA TN D-3151, 1965.

11. Frost, N. E.; and Dugdale, D. S.: The Propagation of Fatigue Cracks in Sheet Specimens. J. Mech. Phys. Solids, vol. 6, no. 2, 1958, pp. 92-110.

12. Liu, H. W.: Fatigue Crack Propagation and Applied Stress Range – An Energy Approach. Trans. ASME, Ser. D: J. Basic Eng., vol. 85, no. 1, Mar. 1963, pp. 116-122.

13. Liu, H. W.: Fatigue Crack Propagation and the Stresses and Strains in the Vicinity of a Crack. Appl. Mater. Res., vol. 3, no. 4, Oct. 1964, pp. 229-237.

14. McEvily, A. J., Jr.; and Boettner, R. C.: On Fatigue Crack Propagation in F.C.C. Metals. Acta Met., vol. 11, no. 7, July 1963, pp. 725-743.

15. Kuhn, Paul: Notch Effects on Fatigue and Static Strength. Current Aeronautical Fatigue Problems, J. Schijve, J. R. Heath-Smith, and E. R. Welbourne, eds., Pergamon Press, c.1965, pp. 229-264.

16. Dixon, J. R.: Stress Distribution Around a Central Crack in a Plate Loaded in Tension; Effect of Finite Width of Plate. J. Roy. Aeron. Soc., vol. 64, no. 591, Mar. 1960, pp. 141-145.

TABLE I.- MATERIAL DESCRIPTION

(a) Average longitudinal and transverse tensile properties of the Ti-8Al-1Mo-1V (duplex-annealed) specimens tested

Grain direction	σ_u, ksi (MN/m^2)	σ_y, ksi (MN/m^2)	E, ksi (GN/m^2)	e, percent	Number of tests
Longitudinal	150.0 (1034)	136.1 (938)	17.3×10^3 (119)	13.2	6
Transverse	149.2 (1029)	135.3 (933)	16.9×10^3 (117)	11.2	3

(b) Nominal chemical composition of Ti-8Al-1Mo-1V

[Values given in percent]

C	Mo	V	Al	N	H	Ti	Fe
0.08 max.	0.75 to 1.25	0.75 to 1.25	7.50 to 8.50	0.05 max.	0.015 max.	Balance	0.30 max.

(c) Condition for duplex annealing

(1) Heat material to 1450° F (1061° K) for 8 hours.
(2) Furnace cool.
(3) Heat to 1450° F (1061° K) for 15 minutes.
(4) Air cool.

TABLE II.- MEAN NUMBER OF CYCLES REQUIRED TO EXTEND CRACKS FROM A HALF-LENGTH a OF 0.15 INCH (0.38 cm)

$[S'_m = 25$ ksi $(173$ MN/m$^2)]$

S'_a		Number of cycles required to propagate a crack from a half-length a of 0.15 in. (0.38 cm) to a half-length a of:													
ksi	MN/m^2	0.20 in. (0.508 cm)	0.30 in. (0.762 cm)	0.40 in. (1.016 cm)	0.50 in. (1.270 cm)	0.60 in. (1.524 cm)	0.70 in. (1.778 cm)	0.80 in. (2.032 cm)	0.90 in. (2.286 cm)	1.00 in. (2.540 cm)	1.20 in. (3.048 cm)	1.40 in. (3.556 cm)	1.60 in. (4.064 cm)	1.80 in. (4.572 cm)	2.00 in. (5.080 cm)
2-inch-wide (5.12-cm) specimens															
25	173	1 750	4 100	5 200											
15	104	3 700	8 200	11 100											
10	69	7 800	17 300	23 000											
[a]5	35	80 000	162 000	201 000	220 000										
[b]2	14	1 260 000	2 370 000	2 820 000	3 020 000										
4-inch-wide (10.2-cm) specimens															
25	173	1 750	3 800												
15	104	3 500	9 100	12 100	14 000	15 900									
10	69	7 800	18 000	25 000	29 700	33 000	36 000	38 300							
5	35	38 000	81 000	111 000	133 000	148 000	160 000	169 000	177 000						
[b]2	14	810 000	1 290 000	1 450 000	1 560 000	1 645 000	1 700 000	1 750 000	1 780 000						
8-inch-wide (20.3-cm) transverse-grain specimens															
25	173	1 300	2 900												
15	104	3 700	8 600	11 100											
10	69	7 750	16 800	23 800	28 800	32 500	34 900								
[a]5	35	35 000	92 000	132 000	158 000	176 000	189 000	199 000	207 000	214 000	223 000	228 000			
[b]2	14	340 000	750 000	1 000 000	1 170 000	1 310 000	1 420 000	1 520 000	1 590 000	1 650 000	1 740 000	1 810 000	1 860 000		
8-inch-wide (20.3-cm) longitudinal-grain specimens (ref. 7)															
25	173	1 750	3 700	4 900											
15	104	4 300	10 500	14 300	17 000										
10	69	8 000	19 500	28 000	34 000	38 500	42 000	45 000							
5	35	75 000	155 000	200 000	240 000	265 000	285 000	300 000	310 000	320 000	330 000				
[b]2	14	660 000	1 800 000	2 645 000	3 280 000	3 700 000	4 020 000	4 280 000	4 460 000	4 590 000	4 770 000	4 900 000	4 980 000	5 050 000	
20-inch-wide (50.8-cm) specimens															
25	173	960	2 080	2 750	3 140	3 430	3 600	3 730	3 830						
15	104	2 800	7 000	9 600	11 700	13 150	14 300	15 300	16 000	16 550	17 350	17 800	18 000		
10	69	6 500	15 800	22 500	27 600	31 600	34 500	36 900							
[a]5	35	42 000	100 000	138 000	165 000	186 000	202 000	215 000	225 000	234 000	249 000	261 000	270 000	278 000	285 000
[b]2	14	270 000	750 000	1 080 000	1 275 000	1 430 000	1 550 000	1 665 000	1 755 000	1 830 000	1 950 000	2 050 000	2 130 000	2 190 000	2 245 000

[a]Crack initiated at S'_a of 10 ksi (69 MN/m^2) to expedite testing.

[b]Crack initiated at S'_a of 5 ksi (35 MN/m^2) to expedite testing.

TABLE III.- SUMMARY OF TRANSITION CRACK LENGTHS

S'_a		2a at transition		Type of shear
ksi	MN/m^2	in.	cm	
2-inch-wide (5.1-cm) specimens				
25	173	0.33	0.84	Double
15	104	.62	1.58	Single
10	69	----	----	None
5	35	----	----	None
2	14	----	----	None
4-inch-wide (10.2-cm) specimens				
25	173	0.35	0.89	Dual
15	104	.75	1.91	Dual
10	69	.92	2.34	Single
5	35	----	----	None
2	14	----	----	None
8-inch-wide (20.3-cm) transverse-grain specimens				
25	173	0.27	0.69	Dual
15	104	----	----	None
10	69	1.32	3.35	Single
5	35	----	----	None
2	14	----	----	None
8-inch-wide (20.3-cm) longitudinal-grain specimens				
25	173	0.20	0.51	Single
15	104	1.02	2.59	Dual
10	69	1.20	3.05	Dual
5	35	1.33	3.38	Single
2	14	----	----	None
20-inch-wide (50.8-cm) specimens				
25	173	0.36	0.91	Double
15	104	.46	1.17	Single
10	69	1.05	2.67	Single
5	35	3.11	7.90	Single
2	14	6.75	17.15	Double

"The aeronautical and space activities of the United States shall be conducted so as to contribute . . . to the expansion of human knowledge of phenomena in the atmosphere and space. The Administration shall provide for the widest practicable and appropriate dissemination of information concerning its activities and the results thereof."

—NATIONAL AERONAUTICS AND SPACE ACT OF 1958

NASA SCIENTIFIC AND TECHNICAL PUBLICATIONS

TECHNICAL REPORTS: Scientific and technical information considered important, complete, and a lasting contribution to existing knowledge.

TECHNICAL NOTES: Information less broad in scope but nevertheless of importance as a contribution to existing knowledge.

TECHNICAL MEMORANDUMS: Information receiving limited distribution because of preliminary data, security classification, or other reasons.

CONTRACTOR REPORTS: Technical information generated in connection with a NASA contract or grant and released under NASA auspices.

TECHNICAL TRANSLATIONS: Information published in a foreign language considered to merit NASA distribution in English.

TECHNICAL REPRINTS: Information derived from NASA activities and initially published in the form of journal articles.

SPECIAL PUBLICATIONS: Information derived from or of value to NASA activities but not necessarily reporting the results of individual NASA-programmed scientific efforts. Publications include conference proceedings, monographs, data compilations, handbooks, sourcebooks, and special bibliographies.

Details on the availability of these publications may be obtained from:

SCIENTIFIC AND TECHNICAL INFORMATION DIVISION

NATIONAL AERONAUTICS AND SPACE ADMINISTRATION

Washington, D.C. 20546